Substrate Resistance Extraction Using a Multi-domain Surface Integral Formulation

Anne Vithayathil
Dept. of Electrical Engineering
and Computer Science
Massachusetts Institute of Technology
Cambridge, MA 02139
Email: anniev@mit.edu

Xin Hu
Dept. of Electrical Engineering
and Computer Science
Massachusetts Institute of Technology
Cambridge, MA 02139
Email: xinhu@mit.edu

Jacob White
Dept. of Electrical Engineering
and Computer Science
Massachusetts Institute of Technology
Cambridge, MA 02139
Email: white@mit.edu

***Abstract*— In order to assess and optimize layout strategies for minimizing substrate noise, it is necessary to have fast and accurate techniques for computing contact coupling resistances associated with the substrate. In this paper, we describe an extraction method capable of full-chip analysis which combines modest geometric approximations, a novel integral formulation, and an FFT-accelerated preconditioned iterative method.**

I. Introduction

In order to assess and optimize layout strategies for minimizing substrate noise, it is necessary to have fast and accurate techniques for computing contact coupling resistances associated with the substrate. To properly extract the substrate coupling resistances, it is necessary to solve the three-dimensional Poisson's equation for fairly complicated geometries of conductors on the surface of a multilayer substrate. A number of methods have been developed to address this problem, including fast integral equation methods with multilayer Green's functions [2] and finite difference techniques [3], but they are either not efficient enough to handle an entire integrated circuit layout or difficult to implement.

In this paper, we describe an extraction method capable of full-chip analysis which combines modest geometric approximations, a novel integral formulation, and an FFT-accelerated preconditioned iterative method. In particular, we model the effects of non-zero conductances in the substrate by considering a multilayer, rectangular substrate slab where each layer has a homogeneous conductivity. The device to substrate contacts are located on a bulk substrate with a thin epitaxial layer. The substrate configuration is shown in Figure 1. It should be noted that the formulation is easily extensible to more general multilayered problems and is straightforward to implement.

We conclude this paper with numerical results from a C++ implementation of the algorithm. These results show favorable convergence and performance for different excitations.

II. Formulation

A. Geometry

In order to keep the extraction problem tractable, we assume a two-block rectangular substrate slab as shown in Figure 1 with different upper and lower conductivities and varying

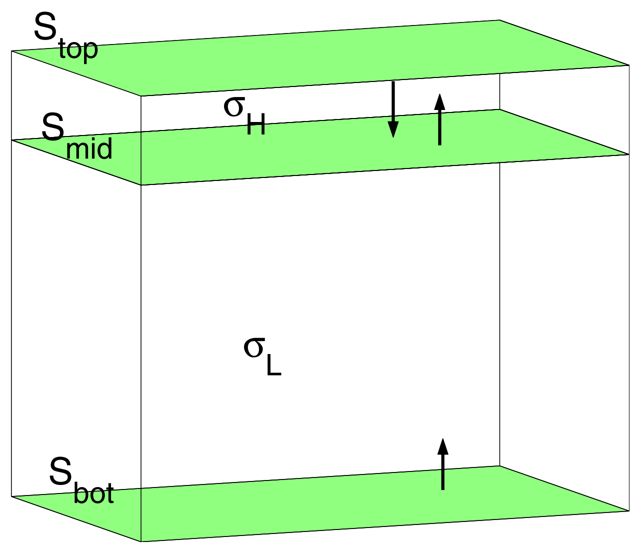

Fig. 1. Geometry of a two-layered substrate

top surface contact locations. Similar to the surface integral formulation developed in [1], our problem is approached using a system of surface integral equations that is coupled through current conservation at the planar interfaces between layers. The accuracy of the formulation rests on the assumption that the contacts are far enough from the sides of the substrate that the potential on the substrate's side surfaces make negligible contributions to the overall potentials in the substrate.

B. Surface Integral Formulation

Applying Green's theorem [1] to this problem yields the following approximate system of integral equations that relates surface potentials to surface electric fields in the upper and lower blocks:

$$\phi_u(r) = -\int_{S_{top}\cup S_{mid}} G(r,r')\frac{\partial \phi_u(r')}{\partial n}dr' + \int_{S_{top}\cup S_{mid}} \phi_u(r')\frac{\partial G(r,r')}{\partial n}dr' \quad (1)$$

and

$$\phi_l(r) = \int_{S_{mid}\cup S_{bot}} G(r,r')\frac{\partial \phi_u(r')}{\partial n}dr' - \int_{S_{mid}\cup S_{bot}} \phi_u(r')\frac{\partial G(r,r')}{\partial n}dr', \qquad (2)$$

with Green's function G defined as:

$$G(r,r') = \frac{1}{4\pi|r-r'|}. \qquad (3)$$

In equations(1) and (2), ϕ_u and ϕ_l are the electric potentials in the upper and lower blocks of the substrate, respectively, and $\frac{\partial \phi_u}{\partial n}$ and $\frac{\partial \phi_l}{\partial n}$ are the surface normal electric fields for the upper and lower blocks, respectively. S_{top}, S_{mid} and S_{bot} are the three surface layers indicated in Figure 1. For clarification, the orientation of the surface normals are shown in Figure 1.

Equations (1) and (2) are coupled through the continuity relations at S_{mid}, which interfaces the upper and lower blocks. These continuity relations are:

$$\phi_u(r) = \phi_l(r) \quad r \in S_{mid} \qquad (4)$$

and

$$\sigma_H \frac{\partial \phi_u(r)}{\partial n} = \sigma_L \frac{\partial \phi_l(r)}{\partial n}, \quad r \in S_{mid} \qquad (5)$$

where σ_H and σ_L are the conductivities of the upper and lower blocks, respectively.

By using the continuity relations, ϕ_l and $\frac{\partial \phi_l}{\partial n}$ at S_{mid} can be eliminated from equation(2). The final system of equations is then given by:

$$\phi_u(r) = -\int_{S_{top}} G(r,r')\frac{\partial \phi_u(r')}{\partial n}dr' - \int_{S_{mid}} G(r,r')\frac{\partial \phi_u(r')}{\partial n}dr' + \int_{S_{top}} \frac{\partial G(r,r')}{\partial n}\phi_u(r')dr' + \int_{S_{mid}} \frac{\partial G(r,r')}{\partial n}\phi_u(r')dr' \qquad (6)$$

and

$$\phi_l(r) = \alpha \int_{S_{mid}} G(r,r')\frac{\partial \phi_u(r')}{\partial n}dr' + \int_{S_{bot}} G(r,r')\frac{\partial \phi_l(r')}{\partial n}dr' - \int_{S_{mid}} \frac{\partial G(r,r')}{\partial n}\phi_u(r')dr' - \int_{S_{bot}} \frac{\partial G(r,r')}{\partial n}\phi_l(r')dr'. \qquad (7)$$

In equation (7), the conductivity ratio α is the ratio of σ_H to σ_L. Dirichlet or Neumann boundary conditions, or a mix of both, are specified for the top and bottom surfaces of the substrate.

C. Equation Summary

Overall, the system contains four integral equations and two boundary conditions. The two boundary conditons are:

$$a(r)\phi_u(r) + b(r)\frac{\partial \phi_u(r)}{\partial n} = f_1(r), r \in S_{top}, \qquad (8)$$

where for each position on the top surface, $(r) = 1$ and $b(r) = 0$ if r is on a metal contact; $b(r) = 1$ otherwise. The function $f(r) = 0$ if r is not on a metal contact and is either one or zero depending on the coupling resistance being computed, and

$$c\phi_l(r) + d\frac{\partial \phi_l(r)}{\partial n} = f_2(r), r \in S_{bot} \qquad (9)$$

where $c = 1$, $d = 0$ for a grounded backside substrate and $c = 0$, $d = 1$ for and insulated backside.

The four integral equations are:

$$\phi_u(r) = -\int_{S_{top}} G(r,r')\frac{\partial \phi_u(r')}{\partial n}dr' - \int_{S_{mid}} G(r,r')\frac{\partial \phi_u(r')}{\partial n}dr' + \int_{S_{top}} \frac{\partial G(r,r')}{\partial n}\phi_u(r')dr' + \int_{S_{mid}} \frac{\partial G(r,r')}{\partial n}\phi_u(r')dr' \quad r \in S_{top}, \qquad (10)$$

$$\phi_u(r) = -\int_{S_{top}} G(r,r')\frac{\partial \phi_u(r')}{\partial n}dr' - \int_{S_{mid}} G(r,r')\frac{\partial \phi_u(r')}{\partial n}dr' + \int_{S_{top}} \frac{\partial G(r,r')}{\partial n}\phi_u(r')dr' + \int_{S_{mid}} \frac{\partial G(r,r')}{\partial n}\phi_u(r')dr' \quad r \in S_{mid}, \qquad (11)$$

$$\phi_l(r) = \alpha \int_{S_{mid}} G(r,r')\frac{\partial \phi_u(r')}{\partial n}dr' + \int_{S_{bot}} G(r,r')\frac{\partial \phi_l(r')}{\partial n}dr' - \int_{S_{mid}} \frac{\partial G(r,r')}{\partial n}\phi_u(r')dr' - \int_{S_{bot}} \frac{\partial G(r,r')}{\partial n}\phi_l(r')dr' \quad r \in S_{mid}, \qquad (12)$$

$$\phi_l(r) = \alpha \int_{S_{mid}} G(r,r')\frac{\partial \phi_u(r')}{\partial n}dr' + \int_{S_{bot}} G(r,r')\frac{\partial \phi_l(r')}{\partial n}dr' - \int_{S_{mid}} \frac{\partial G(r,r')}{\partial n}\phi_u(r')dr' - \int_{S_{bot}} \frac{\partial G(r,r')}{\partial n}\phi_l(r')dr' \quad r \in S_{bot}. \qquad (13)$$

In the above equations,
$\phi_{top} = \phi_u(r), r \in S_{top}$, $\frac{\partial \phi_{top}}{\partial n} = \frac{\partial \phi_u(r)}{\partial n}, r \in S_{top}$
$\phi_{mid} = \phi_u(r), r \in S_{mid}$, $\frac{\partial \phi_{mid}}{\partial n} = \frac{\partial \phi_u(r)}{\partial n}, r \in S_{mid}$
$\phi_{bot} = \phi_l(r), r \in S_{bot}$, $\frac{\partial \phi_{bot}}{\partial n} = \frac{\partial \phi_l(r)}{\partial n}, r \in S_{bot}$

III. Matrix Solution

The top, middle and bottom surface layers are each discretized with an n_x x n_y grid of regular, rectangular panels, generating $3n_xn_y$ total panels. Each panel provides the local support for two piece-wise constant basis functions, one representing a constant $\phi(r)$ on the panel, and the other representing a constant $\frac{\partial \phi(r)}{\partial n}$ on the panel. We will solve for a discretized solution of six unknowns, each unknown is approximated by a weighted sum of these basis functions.

By inserting this discretized representation into Equations (8)-(13) and subsequently testing the equations at the centroids of each panel, a matrix equation is generated. This matrix is

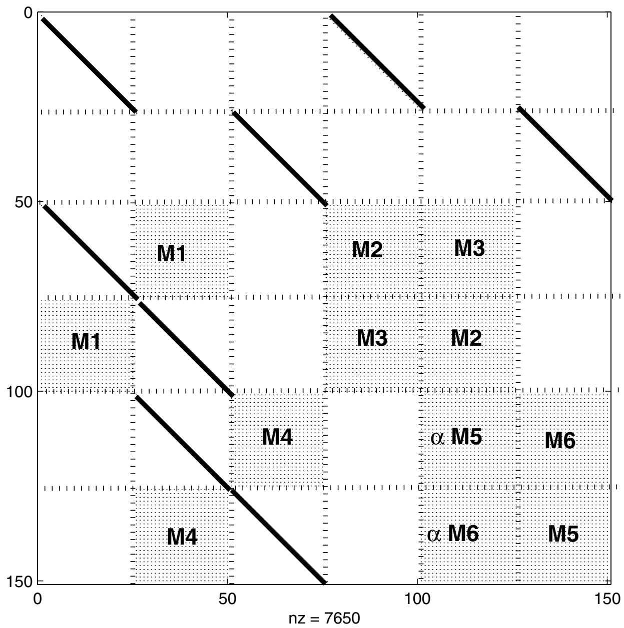

Fig. 2. System Matrix Structure

shown in block form in Figure 2. Note that each submatrix block indicated in the figure is of size $n_x n_y$ x $n_x n_y$. The first two blocked rows of the matrix, which correspond to the boundary conditions tested at the top and bottom surfaces, each have two nonzero diagonal blocks. The third through sixth blocked rows correspond to testing Equations (10)-(13), respectively. The solution vector sought is a column vector, of size $6n_x n_y$, which has a blocked row structure. Each blocked row of size $n_x n_y$ corresponds to the weights in the expansion of either ϕ or $\frac{\partial \phi}{\partial n}$ for a single layer. Our ordering chosen for these blocks is: ϕ_{top},ϕ_{mid}, ϕ_{bot}, $\frac{\partial \phi_{top}}{\partial n}$,$\frac{\partial \phi_{mid}}{\partial n}$,$\frac{\partial \phi_{bot}}{\partial n}$

This matrix equation is solved using a Generalized Conjugate Residual(GCR) iterative method that requires only one matrix-vector product at each iteration. Because of the sparsity pattern of the matrix, a matrix-vector product can be decomposed into submatrix-subvector products. Each of these submatrix-subvector-products is a two-dimensional discrete convolution. Due to the reguarity of the grid, this convolution can be performed in $O(n_x n_y log(n_x n_y))$ operations via FFTs. A right-preconditioner is formed from the diagonals of the submatrices and is used to accelerate the convergence of the GCR algorithm.

IV. Computational Results

Two types of Dirichlet boundary conditions are imposed on the top surface of the substrate to test the convergence rate of the proposed solution. The bottom surface of the substrate is grounded. The first type of boundary condition is to randomly set each discretized panel on the top surface to a potential of either 1V or 0V. The second type of boundary condition is to set the voltages of strips of panels on the top surface to a regular sequence of 1Vs and 0Vs. Tables 1 and 2 contain the convergence and timing results obtained for each boundary condition type at different levels of structural discretization.

Table 1: Convergence and Timing Results for the First Type of Boundary Condition

System matrix	Iteration Count	Total CPU time (s)
3750 X 3750 (25 X 25 $\frac{panels}{layer}$)	20	2.716
33750 X 33750 (75 X 75 $\frac{panels}{layer}$)	31	68.61
93750 X 93750 (125 X 125 $\frac{panels}{layer}$)	88	253.46
183750 X 183750 (175 X 175 $\frac{panels}{layer}$)	45	634.43
453750 X 453750 (275 X 275 $\frac{panels}{layer}$)	56	1772.54
43750 X 843750 (375 X 375 $\frac{panels}{layer}$)	68	5242.21
(475 X 475 $\frac{panels}{layer}$)	73	8461.75

Table 1: Convergence and Timing Results for the Second Type of Boundary Condition

System matrix (s)	Iteration Count	Total CPU time
3750 X 3750 (25 X 25 $\frac{panels}{layer}$)	15	1.98
33750 X 33750 (75 X 75 $\frac{panels}{layer}$)	23	48.83
93750 X 93750 (125 X 125 $\frac{panels}{layer}$)	28	175.34
183750 X 183750 (175 X 175 $\frac{panels}{layer}$)	32	411.64
303750 X 303750 (225 X 225 $\frac{panels}{layer}$)	37	658.72
453750 X 453750 (275 X 275 $\frac{panels}{layer}$)	40	1097.71

V. Conclusions

Experimental results have demonstrated that the iterative method converges in seventy-five iterations or less, even for problems with more than a million unknowns. It can then be concluded that the surface integral formulation with matrix sparsification techniques has solved the substrate coupling problem with accuracy and fast convergence rate. This ”fast” method can be utilized to simulate large substrate coupling problems with a great number of unknowns in an efficient and accurate manner. We are currently implementing extensions to the method to allow for trench isolation.

ACKNOWLEDGMENT

The authors wish to acknowledge support from the National Science Foundation and the MARCO Interconnect Focus Center.

REFERENCES

[1] S. Kuo, M. Altman, J. Bardhan, B. Tidor and J. White. "Fast Methods for Simulation of Biomolecule Electrostatics." *IEEE/ACM Conference on Computer-Aided Design,* June 2002.

[2] M. Niknejad, R. Gharpurey, and R. Meyer. "Numerically Stable Green Function for Modeling and Analysis of Substrate Coupling in Integrated Circuits." *IEEE Trans. on Computer Aided Design of Integrated Circuits and Systems,* vol. 17, no.4, pp. 305-315, April 1998.

[3] N. Verghese and D. Allstot. "Rapid Simulation of Substrate Coupling Effects in Mixed-Mode ICs." *Proc. IEEE Custom Integrated Circuits Conference,* pp. 18.3.1-18.3.4, May 1993.

[4] T. Sakar, E. Arvad and S. Rao. "Application of FFT and the Conjugate Gradient Method for the Solution of Electromagnetic Radiation from Electrically Large and Small Conducting Bodies" *IEEE Trans. Antennas and Propagation,* vol. AP-34, pp. 635-640, 1986.

[5] M. Chou *Fast Algorithm for Ill-Conditioned Dense-Matrix Problems in VLSI Interconnect and Substrate Modeling*. Ph.D. thesis, MIT EECS Department, June 1998.

